Commercial RFIDs as Reconfigurable Intelligent Surfaces

B10202010 吳恩宇
B11901074 李柏宇
B11901064 楊詠翔

Introduction (1/2)

- Reconfigurable Intelligent Surfaces (RISs) is a programmable surface structure that can be used to control the reflection of electromagnetic (EM) waves by changing the electric and magnetic properties of the surface. [1]
- RISs are able to enhance the signal strength. As emerging communication technology tends to have more weakening penetration capability, RIS has become a promising solution to such issues.

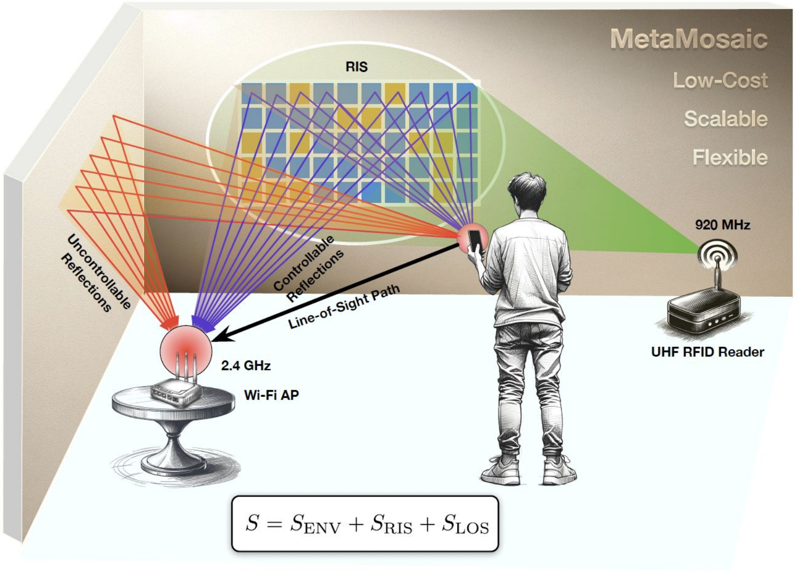

Introduction (2/2)

There're 2 major materials to compose RISs:

1. Metasurface: EM Metasurface is an artificially engineered, two-dimensional material designed to control the behavior of electromagnetic waves through arrays of subwavelength features.
2. Antenna Array: Antenna Array includes electrically tunable reflecting antenna arrays that can be used to dynamically adjust their radiation patterns.

Prior Work (1/3)

	MetaMosaic	F. Lestini et al. (2023) [2]
Type	RFID controlled RIS	RFID controlled RIS
Scale	2,418 elements	2 elements (only a proof-of-concept)
Component	2 antennas, 2 chips, 1 diode, 1 battery	1 antenna, 1 chip, 1 MOSFET
Power	Battery-free	Require Battery
Control	Wireless (RFID)	Wireless (RFID)

Prior Work (2/3)

	MetaMosaic	RFocus [3]
Type	RFID controlled RIS	Wired controlled RIS
Scale	2,418 elements	80 boards
Component	2 antennas, 2 chips, 1 diode, 1 battery	40 antennas per board (custom designed)
Power	Battery-free	Wired power
Control	Wireless (RFID)	Wired
Response Time	49-160 ms	1-10 seconds

Prior Work (3/3)

	MetaMosaic	Vardakis et al. (2022) [4]
Type	RFID controlled RIS	RFID controlled RIS
Scale	2,418 elements	100 elements (proof-of-concept), 256 elements (testbed)
Power Gain	18.82dB average, 25dB peak	~2-3dB for 100 elements
Power	Battery-free	Battery-free
Control	Wireless (RFID)	Wireless (RFID)
Response Time	49-160 ms	43-116 ms (for mere 50 elements)
Operational Freq.	920MHz + 2.4GHz	around 870MHz

Repurposing RFID into Unit Cell

Goal: Convert commercial RFID tags into 1-bit phase-controllable RIS cells.

Use RFID chip for wireless control & energy harvesting at 920 MHz.

Dual-band microstrip patch antenna supports 920 MHz + 2.4 GHz.

Switching load controls reflection phase: Γ = +1 or -1.

Enables low-cost, battery-free, scalable RIS surfaces.

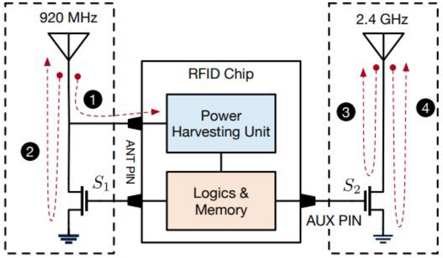

Fig. 3: Design of the unit cell. The unit cell of MetaMosaic composed of a commercial RFID chip and two antennas operating 920MHz and 2.4GHz, respectively.

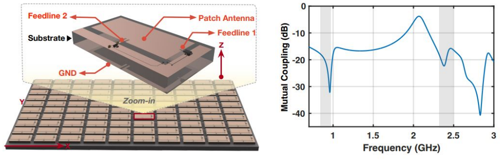

(a) Patch Antenna (b) S_{21}

Fig. 4: Dual-frequency patch antenna. (1) we leverage the dual polarization of path antenna at the two edges to achieve the dual-frequency antenna. (2) shows the mutual coupling coefficient S_{21} of two feed ports.

RIS-NeRF2 Soft-Landing Reconfiguration

Goal: Determine optimal RIS phases efficiently.

Hard-landing issue: 2^M search + slow feedback.

RIS-NeRF2 models environment as voxel radiance field.

Differentiable ray-tracing predicts cell contributions.

Compute best configuration offline → apply instantly.

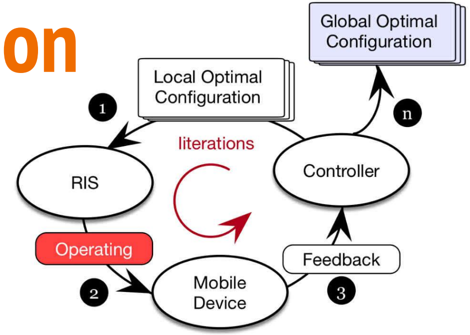

Fig. 5: Hard-landing based Configuration strategy. Past RIS systems adopt the heuristic search algorithm to identify the optimal configuration parameters after multiple iterations. In each iteration, when a new configuration is assumed, the controller necessitates the RX device to constantly provide feedback on the signal strength.

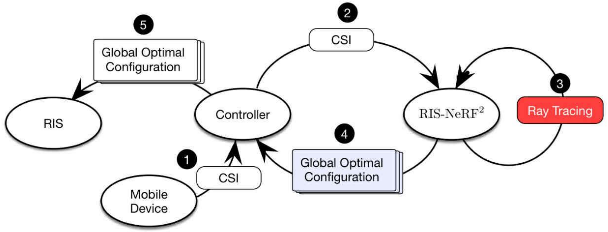

Fig. 9: Soft-landing based Configuration. The efficacy of a proposed configuration can be evaluated by the ray tracing algorithm with RIS-NeRF^2. This approach allows for the assessment of the configuration's impact without actually implementing it on the RIS or necessitating feedback from the TX.

Scene Representation

The environment is represented as a set of voxels, where each voxel stores two things:

Attenuation Property: How much the signal is attenuated when passing through it.

$$h(V_i) = \Delta a(V_i) e^{j\Delta\theta(V_i)} \qquad \delta(V_i) = -\ln(h(V_i)) = -\ln \Delta a(V_i) - j\Delta\theta(V_i)$$

Radiance Property: How it re-emits the signal.

$$S(P_{\mathrm{TX}}, V_i, \omega) = a(V_i) e^{j\theta(V_i)}$$

Neural Radiance Fields — RIS-NeRF

Attenuation Network: $\mathbf{F}_\delta : (V_i) \rightarrow (\delta(V_i), \mathcal{F}(V_i))$

Radiance Network: $\mathbf{F}_\gamma : (P_{\mathrm{TX}}, \mathcal{F}(V_i), \omega) \rightarrow a(V_i)e^{j\theta(V_i)}$

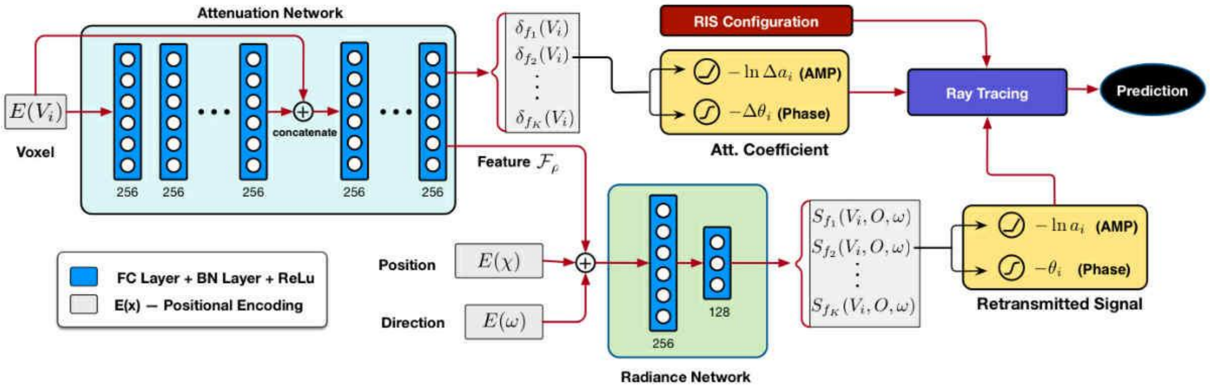

Fig. 6: Network Architecture of RIS-NeRF[2]

Ray Tracing

Tracing from a Singal Voxel:

$$S(\chi, V_N) = \Big(\prod_{m=1}^{N-1} h(V_m)\Big) \cdot S(\chi, V_N, -\omega) = \exp\Big(-\sum_{m=1}^{N-1} \delta(V_m)\Big) \cdot S(\chi, V_N, -\omega)$$

Tracing from a Direction:

$$S(\chi, \omega) = \sum_{n=1}^{N} S(\chi, V_n) = \sum_{n=1}^{N} \Big(\exp\big(-\sum_{m=1}^{n-1} \delta(V_m)\big) \cdot S(\chi, V_n, -\omega)\Big)$$

Tracing from All Directions:

$$S(\chi) = \sum_{\omega \in \Omega} S(\chi, \omega) = \sum_{\omega \in \Omega} \sum_{n=1}^{N} \Big(\exp\big(-\sum_{m=1}^{n-1} \delta(V_m)\big) \cdot S(\chi, V_n, -\omega)\Big)$$

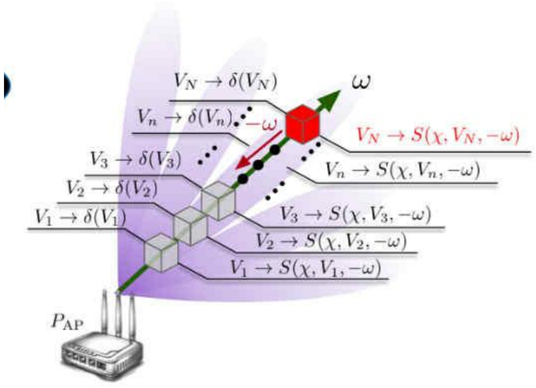

Fig. 7: Ray Tracing

Soft-landing Reconfiguration Algorithm

$$S_{\mathrm{AP}}(\chi) = S_{\mathrm{LOS}}(\chi) + S_{\mathrm{ENV}}(\chi) + S_{\mathrm{RIS}}(\chi) = S_{\mathrm{TRUNK}}(\chi) + S_{\mathrm{RIS}}(\chi)$$

$$S_{\mathrm{RIS}}(\chi) = \sum_{V_i \in \mathcal{V}_{\mathrm{RIS}}} S(\chi, V_i)$$

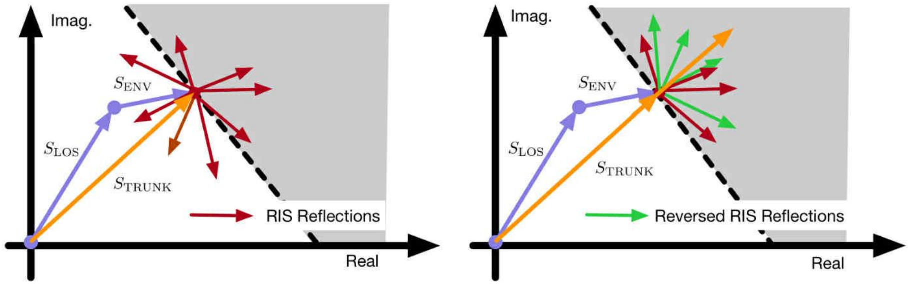

(a) Before Configuration (b) After Configuration

Fig. 8: Configuration Strategy. The orientations of reflections from the unit cells of the RIS are maintained or reversed to ensure alignment with the primary trunk signal

Implementation

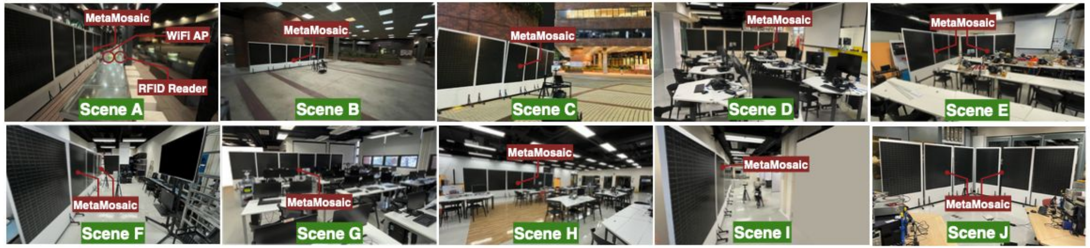

Fig. 10: Illustration of Experimental Scenes

The MetaMosaic system consists of four components: unit cells, surfaces, a controller, and the RIS-NeRF² model.

(1) Unit Cells

Low-cost EM4325 RFID chip with a dual-frequency antenna and passive design, costing under $0.5 per cell and requiring no battery or charging.

(2) Surfaces

Six RIS panels (each 13×31 cells, ~1.2×2 m²) were built, creating a fully modular, scalable, and movable setup for different environments.

(3) Controller

ImpinJ R410 RFID reader wirelessly controls all cells via standard commands, a completely cable-free operation.

(4) RIS-NeRF²

Neural Radiance Field–based model to predict optimal configurations, achieving <10 ms reconfiguration latency after training.

Experimental Result(1/3)

Performance of RIS-NeRF²

RIS-NeRF² enables **fast and accurate** prediction of the best RIS configurations without trial-and-error(hard-landing based configuration).

(1) Accuracy

Trained on data from 284,124 positions across 10 scenes, RIS-NeRF² achieved an average median deviation of **only 0.74%**, with 90% of scenes under 1%, proving **highly precise** channel prediction.

(2) Response Time

Reconfiguration generally 0.05-0.25s across four test scenes, mainly limited by RFID command latency (~0.8 ms each), making it **10× faster** than state-of-the-art systems like RFocus (1–10 s).

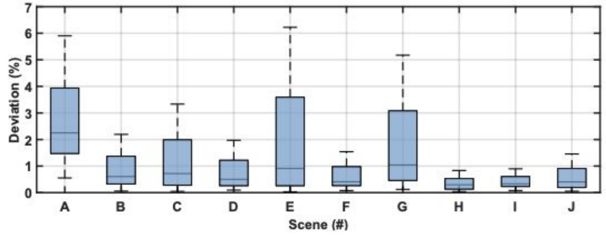

Fig. 11: Accuracy of RIS-NeRF²

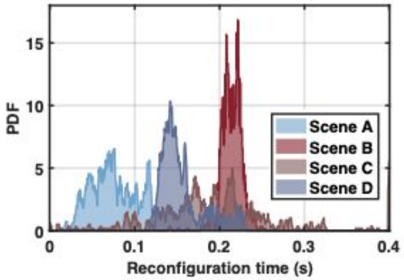

Fig. 13: Response Time

Experimental Result(2/3)

Overall Performance

(1) Gain Across Scenes

MetaMsaoic boosted Wi-Fi signal strength with an **average median gain of 18.82 dB**, proving **strong and reliable enhancement** in both semi-indoor and indoor settings. The large gain comes from two reasons:

1. each surface is fully reflective.
2. precisely aligns reflections, minimizing destructive interference.

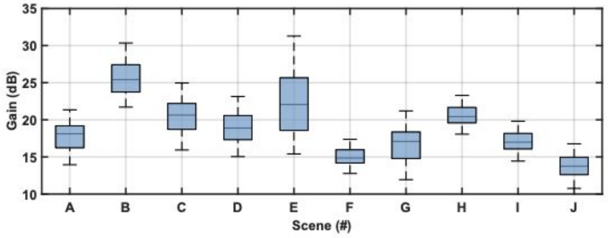

Fig. 12: Gain vs. scenario

(2) Comparison to State-of-the-Art (RFocus)

MetaMosaic achieved **4.6 – 11.7 dB higher** median gain and a better consistent.

MetaMosaic's : stable Gaussian distribution

RFocus : irregular, high-variance behavior

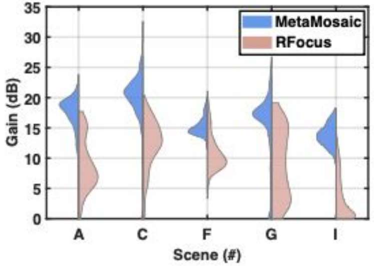

Fig. 14: RFocus vs. MetaMosaic

Experimental Result(3/3)

(3) Scalability

By testing subsets of 600 → 1200 → 1800 → 2400 cells, MetaMosaic showed a steady **gain rise from 8.6 dB to 21.9 dB**, proving that even with 25% tag loss it still maintains ≈ 85% of maximum performance, demonstrating strong **scalability and robustness**.

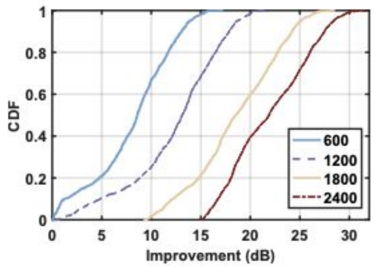

Fig. 15: Scalability

(4) Impact of Layout

Different cell arrangements—linear, L-shaped, X-shaped, square, and random—changed the gain by **less than 2 dB**, with the random pattern slightly best (4.3 dB), confirming MetaMosaic's layout-independent **flexibility and easy deployment**.

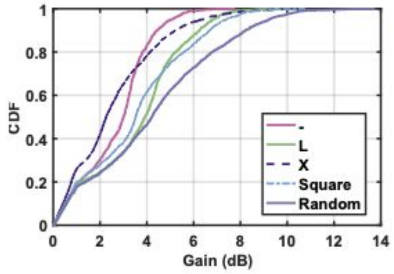

Fig. 16: Layout

Field Study: XR Booster

Setup

A PC (AP mode) streamed data to a HoloLens 2 headset, while the user moved every 30 seconds; throughput and latency were measured using iperf and ping over 14 minutes.

Results

With MetaMosaic: **14.86 Mbps** throughput.

Without: **5.66 Mbps** (a 2.6× improvement)

Latency: reduce from 10.07 ms to 4.63 ms (−54%).

Interpretation

The system meets Ericsson's XR benchmarks—tens of Mbps and <20 ms latency—demonstrating that MetaMosaic enables **reliable, high-speed XR** communication.

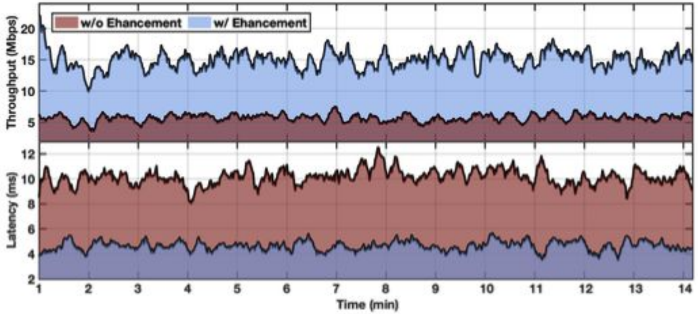

Fig. 17: Throughput and Latency in the Field Study

Impact of MetaMosaic (1/3)

Research Impact:

- MetaMosaic proves that RIS can be built from commercial RFID by hands-on experiments and real-world testcase.
- MetaMosaic extends the prior proof-of-concept RFID controlled RIS research into a scalable, pratical and effective RIS solution.
- MetaMosaic validates their RIS-NeRF^2 optimization at commercial scale with 0.74% prediction accuracy and 10× faster reconfiguration than iterative methods.

Impact of MetaMosaic (2/3)

Industry Adoption:

- In their field study, MetaMosaic achieve 2.6× throughput improvement and 54% latency reduction for 2.4GHz Wi-Fi, proving the immediate commercial viability
- Eliminates deployment barriers through wireless control (no wiring), battery-free operation (no maintenance), and flexible layouts, lowering CAPEX/OPEX (資本支出, 營業費用)
- MetaMosaic ulitilizes commercial available components, which enable immediate real-world application without extra design expense

Impact of MetaMosaic (3/3)

Possible Standardization:

- RIS ETSI (歐洲電信標準協會) Industry Specification Groups (ISG)
- 3GPP Release 20/21(6G standard)

Possible User Scenario:

- Home Enviroment: number of APs is limited
- Department Store: LoS transmission is often blocked
- Hall: The setup of APs is limited

References

1. Editorial Team. (2022, December 13). What are Reconfigurable Intelligent Surfaces?. everything RF.
2. F. Lestini, G. Marrocco and C. Occhiuzzi, "Feasibility of RFID-Based Control of Reconfigurable Intelligent Surfaces (RISs) for Wireless Communication Systems," 2023 IEEE 13th International Conference on RFID Technology and Applications (RFID-TA), Aveiro, Portugal, 2023, pp. 241-244, doi: 10.1109/RFID-TA58140.2023.10290619.
3. Venkat Arun and Hari Balakrishnan. 2020. RFocus: beamforming using thousands of passive antennas. In Proceedings of the 17th Usenix Conference on Networked Systems Design and Implementation (NSDI'20). USENIX Association, USA, 1047–1062.
4. I. Vardakis, G. Kotridis, S. Peppas, K. Skyvalakis, G. Vougioukas and A. Bletsas, "Intelligently Wireless Batteryless RF-Powered Reconfigurable Surface: Theory, Implementation & Limitations," in IEEE Transactions on Wireless Communications, vol. 22, no. 6, pp. 3942-3954, June 2023, doi: 10.1109/TWC.2022.3222733.

分工

吳恩宇: Repurposing RFID into Unit Cell ~ Soft-landing Reconfiguration Algorithm

李柏宇: Implementation ~ Field Study: XR Booster

楊詠翔: Introduction, Prior Work and Impact of MetaMosaic